Journal of Composites and Compounds 5 (2023) 153-158

Available online at www.jourcc.com

Journal homepage: www.JOURCC.com

Journal of Composites and Compounds

The computational study of epoxy-based nanocomposites electromechanical performance under external force: Molecular dynamics approach

Peyman Torkian [a, *], *Hamid Baseri* [a]

[a] *Department of Mechanical Enigineering, Babol Noshirvani University of Technology, Babol, Iran*

ABSTRACT

Gauge factor is a measure of the sensitivity of a material's electrical performance to mechanical strain. This property of nanocomposites is important for their usage in various electromechanical applications. In current research, we introduce the electromechanical and gauge factor evolutions of epoxy-graphite/boron nitride (BN) nanocomposites. The molecular dynamics (MD) approach implemented for numerical analyzing of various modeled systems. Computationally, the atomic interactions between particles inside structures described by UFF, and TERSOFF force-fields. After MD simulation settings done, various physical parameters such as temperature, potential energy, interaction energy and gauge factor reported to describe atomic behavior of designed nanocomposites. MD results predicted the physical stability of modeled systems at 300 K as initial temperature (after 10 ns). Also, gauge factor of nanocomposites converged to 3.19 and 6.54 values by graphite and BN inserting to base matrix, respectively. These results indicated by changes nanoparticles type inside epoxy-based nanocomposites, the electromechanical performance of them can be manipulated in actual cases.

Peer review under responsibility of UGPH.

ARTICLE INFORMATION

Article history:
Received 9 March 2023
Received in revised form 22 June 2023
Accepted 10 July 2023

Keywords:
Gauge factor
Graphite
Boron nitride
Nanocomposite
Molecular dynamics
Atomic modeling

Nomenclature

k,	Boltzmann constant;
v,	atomic velocity;
r_c,	cut-off parameter;
r,	interatomic distance;
T,	temperature;
k_r,	energy constant;
r_0,	equilibrium distance;
H,	Hamiltonian;
E,	total energy;
V,	potential energy;
P,	atomic momentum;

Greek symbols

ε,	energy parameter in Lennard-Jones formalism;
σ,	length parameter Lennard-Jones formalism;
k_θ,	rotational energy constant;
θ_0,	equilibrium angle;
Δt,	time step;

1. Introduction

The gauge factor (or strain factor) of a strain gauge is the ratio of relative change in electrical resistance R, to the mechanical strain ε. Strain gauge is a promising sensor implemented for the estimation of physical quantities such as stress, strain, and etc. [1]. Physically, performance of strain gauge parameter is based on piezo-resistance phenomenon [2-4]. So, this parameter also called piezo-resistive gauge. When a metallic samples is compressed/expanded, the size of pristine sample varied. Change in size means change in radius/length of the conductor. Furthermore, the electrical resistance of conductor is related to their length and area of cross-section, therefore a size variation of conductor will cause a change in the electrical resistance of them [5, 6]. Also, it has been detected that the electrical resistance of conductor-based systems also changes due to strain in pristine sample (piezo-resistive Effect) [7].

In actual cases, piezoelectric nanoparticles adding to polymeric matrixes cause gauge-based nanocomposites. Nanocomposite is a multiphase sample where one of the phases has nano-scale size [8, 9]. The electrical composite/nanocomposite structures attracted appreciable attention of researchers in recent years for various applications [10-13]. The main idea behind these structures is to implementing building units with low size to produce new structures with high flexibility and improvement in their thermo-mechanical behaviors [14, 15]. In the sim-

* *Corresponding author: Peyman Torkian; E-mail: peymant69@yahoo.com*

https://doi.org/10.61186/jcc.5.3.1

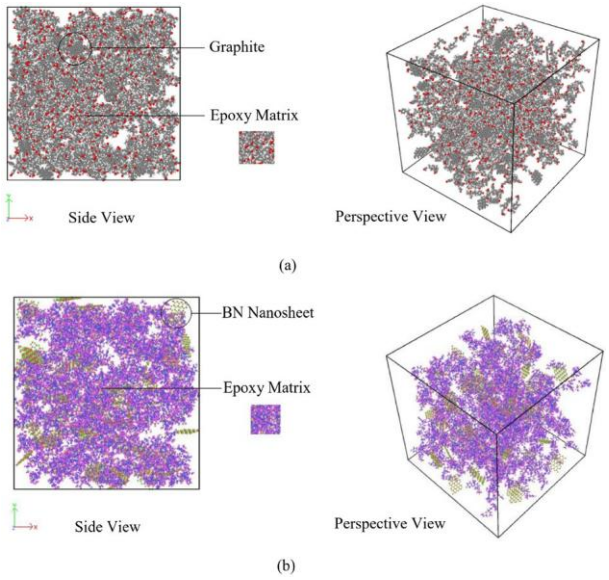

Fig. 1. Schematic of atomic structure of (a) epoxy-graphite and (b) epoxy-BN nanocomposites at initial time step of MD simulations.

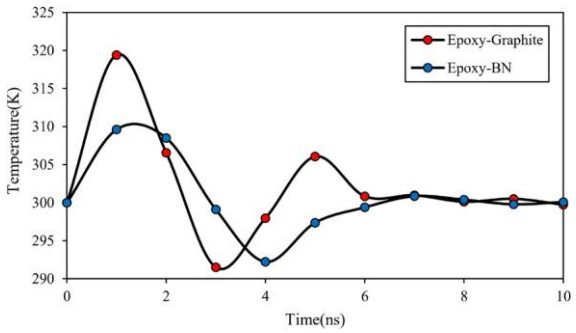

Fig. 2. The temperature variation of epoxy-graphite and epoxy-BN nanocomposites as a function of MD time.

plest case, inserting nanoparticles to polymer-based matrixes (with optimum value) can improve its physical behavior, often dramatically, by capitalizing on the nature and properties of the nanoparticles [16]. This method is promising in yielding high performance compounds, when uniform dispersion of the nanoparticles is implemented and the properties of the nanoparticles are better than those of the pristine sample [17]. In previous researches, the gauge factor of various nanocomposites reported via experimental/numerical approaches. James et al. [18] developed a simple approach which outputs in equations for nanocomposite gauge factors as a function of electrical conductivity of pristine sample and filler value. Their introduced formalism used to fit experimental results with certain physical theorem reported before. They indicated these formalisms to fit experimental outputs, both measured parameters in their work or extracted from previous researches, very well. Importantly, their model indicated the response of sample strain detectors to be more complex than previously thought and shows parameters other than the influence of strain ratio on the inter-particle resistance to be behavior limiting.

In other work, Ren et al. [19] used a computational model based on FE approach to describe the mesoscopic piezo-resistive behavior of polymeric nanocomposites consist of carbon nanotubes (CNTs) as filler. The important parameters that may contribute to the total piezo-resistive react, the CNT piezo-resistivity and the CNT mesoscale network influence are incorporated in the model based on a 3D multiscale mechanical-electrostatic coupled simulator. Their numerical outputs explained how different nanoscale procedures affected the total piezo-resistive performance through the mesoscale nanotubes arrangement. Furthermore, their model described and provided bounds for the wide range of gauge factors found in previous reports offering insight regarding how control of the mesoscale CNT arrangement can be implemented to tailor nanostructure piezo-resistive performance. An et al. [20] introduced the influence of C-based nanoparticles (CNTs) ratio, with various ratio of Triton X-100 as a surfactant on strain detecting in terms of sensitivity and linearity based on electrical resistance outputs. In this research, nanotubes were synthesized via an injection floating catalyst chemical vapor deposition method and their purity detected by Raman spectroscopy and scanning electron. Between various samples, only the pristine sample modified with 0.1 wt.% nanotubes exhibited acceptable piezo-resistivity for the resistance detection, and those with 0.01 wt.% nanotubes did not show measurable conductivity so were excluded in their study, since their CNTs were highly entangled, and conductive network failed to be established. Numerically, they reported with 0.1 wt.% nanoparticles, adding 0.5% content of the surfactant enlarged gauge factor, appreciably. Researchers reported a drop of gauge factor by the order of two by using surfactant with more atomic ratio. Therefore, by comparing the electric conductivity variation between 1.0% and 0.5% surfactant, they supposed that the relatively high surfactant ratio has reached critical micelle concentration, and disrupts the arrangement of CNTs inside pristine matrix.

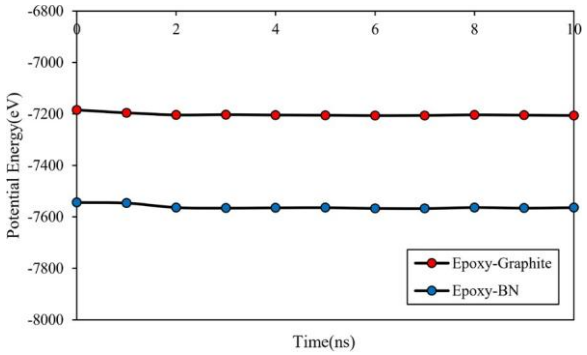

Fig. 3. The potential energy variation of epoxy-graphite and epoxy-BN nanocomposites as a function of MD time.

As reported in previous researches, in addition to experimental methods, computational approaches such as Molecular Dynamics (MD) simulation can be used to describing of polymeric-based nanocomposites physical behavior [21-23]. Currently, we introduced the epoxy-graphite and epoxy- boron nitride (BN) nanocomposites for electromechanical applications by using MD approach for the first time. In these samples, epoxy and graphite/BN compounds regarded as matrix and nanoparticle elements, respectively. We expected MD outputs can be used for optimized procedures designing in various industrial applications (based electrochemical process) in standard condition.

2. MD Simulations Details

In our simulation work, we implemented MD approach to explore electromechanical behavior of epoxy-graphite and epoxy-BN nanocomposites through Large-scale Atomic/Molecular Massively Parallel Simulator (LAMMPS) [24-26]. To build the initial atomic configuration, we used the Avogadro and PACKMOL software [27, 28]. We represent the schematic view of the designed atomic systems with these modeling packages in Fig. 1. To get the reliable results from MD simulations, one should choose atomic potential based on the physical properties under study [29]. In MD descriptions of epoxy-graphite and epoxy-BN nanocomposites, interatomic potentials were based on a UFF and TERSOFF force-fields [30-32]. In UFF force-field, Lennard-Jones (LJ) equation used to describe the non-bond forces between modeled atoms as below [33],

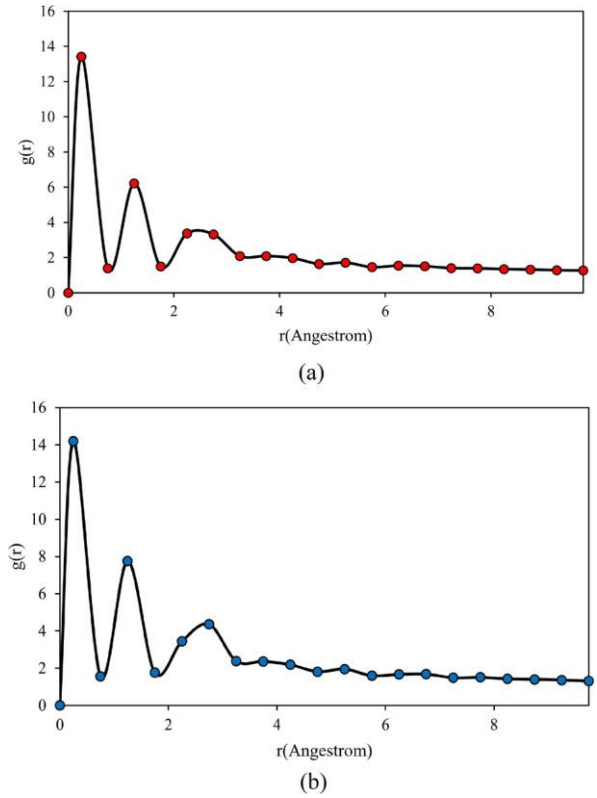

Fig. 4. The RDF of (a) epoxy-graphite and (b) epoxy-BN nanocomposites after equilibrium phase detection in these structures.

$$\phi\left(r_{ij}\right)=4\varepsilon\left[\left(\frac{\sigma}{r_{ij}}\right)^{12}-\left(\frac{\sigma}{r_{ij}}\right)^{6}\right],\ r_{ij}\le r_{c}\ , \tag{1}$$

where, ε constant defines the depth of the energy well, σ constant indicated the atomic distance at which the energy value is zero, and atomic distance between the various particles is set by r_{ij} parameter. The non-bond interaction constants for various atoms listed in **Table 1** [30]. Also, in equation (1), the cut-off radius (r_c) set to 12 Å in all of our calculations. The bond-based forces included the simple bond and angle bond components. Here, the simple/angular bond parameter is defined by harmonic equation as below [34, 35],

$$E_{simple}=\frac{1}{2}K_{r}\left(r-r_{0}\right)^{2} \tag{2}$$

$$E_{angular}=\frac{1}{2}K_{\theta}\left(\theta-\theta_{0}\right)^{2} \tag{3}$$

where, k_r/k_θ is represents the simple/angular energy parameter and r_0/θ_0 defines the atomic bond length/angle. The values of these computational constants in various simulated structures used from UFF force-field [30]. Moreover, we used TERSOFF force-field to BNC-based

Table 1.
The ε and σ parameters value for LJ interactions for various atoms in epoxy-graphite and epoxy-BN nanocomposites [27].

Atom Type	σ Constant(Å)	ε Constant(kcal/mol)
C	3.851	0.105
H	2.886	0.354
O	3.500	0.658
N	3.660	0.700
B	4.083	0.838
Cl	3.947	1.044

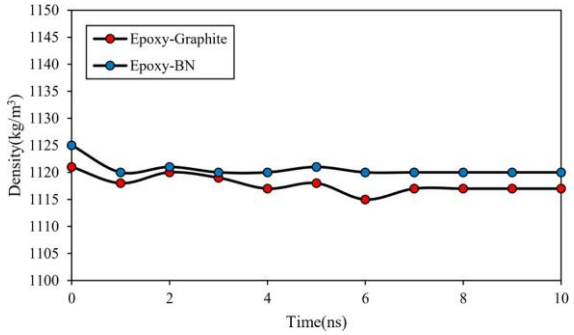

Fig. 5. The density variation of epoxy-graphite and epoxy-BN nanocomposites as a function of MD time.

structures (graphite and BN samples). This interatomic potential formulated as below [31],

$$E=\frac{1}{2}\sum_{i}\sum_{j\neq i}V_{ij} \tag{4}$$

$$V_{ij}=f_{c}\left(r_{ij}\right)\left[f_{R}\left(r_{ij}\right)+b_{ij}f_{A}\left(r_{ij}\right)\right] \tag{5}$$

in equation (5), f_R is a 2-body parameter and f_A is a 3-body parameter in TERSOFF force-field. The summations in TERSOFF relation are overall atomic neighbors within a cutoff radius. Computational ensemble is another important parameter in MD simulations [36]. Technically, by using various ensembles, initial condition can be implemented to simulated structure. In our MD study, NVT ensemble used to setting the system temperature at initial value (T_0). In this algorithm, equations (6) and (7) implemented for "F" physical parameter calculation [37, 38],

$$f\left(N.V.T\right)=\left[N!Q\left(N.V.T\right)\right]^{-1}\int dr^{N}\int dp^{N}\exp\left[\frac{-H\left(r^{N}.p^{N}.V\right)}{KT}\right]F\left(r_{N}.p_{N}.V\right) \tag{6}$$

and,

$$Q\left(N.V.T\right)=\left(N!\right)^{-1}\int dr^{N}\int dp^{N}\exp\left[\frac{-H\left(r^{N}.p^{N}.V\right)}{KT}\right] \tag{7}$$

in equations (6) and (7), N is particles number, V is volume of total system, H is Hamiltonian function, p is pressure, and K represent the Boltzmann constant. Also, the velocity Verlet algorithm used to association of motion relations and evolution of each atoms by MD time steps passing [39-41]. By using these computational descriptions, MD approach in current work consists of two main steps:

STEP A: Firstly, epoxy-graphite and epoxy-BN nanocomposites simulated inside cubic box with 100 Å length. In current simulations, periodic boundary conditions defined to x and y directions and fixed condition used for z direction [42]. Also, Nose-Hoover (NVT) thermostat was implemented to create thermodynamic equilibration state in modeled system at 300 K for 10 ns.

STEP B: Secondary, the external force (with 0.01 kcal/mol.Å value) implemented to electromechanical behavior analyzing of epoxy-graph-

Table 2.
The gauge factor and interaction energy changes of reinforced epoxy-graphite nanocomposite as a function of nanoparticles ratio.

Nanocomposite Atomic Ratio (%)	Gauge Factor	Interaction Energy (eV)
1	2.06	-341.25
2	2.22	-348.03
3	2.78	-352.28
4.6	3.19	-383.31
5	2.34	-350.82

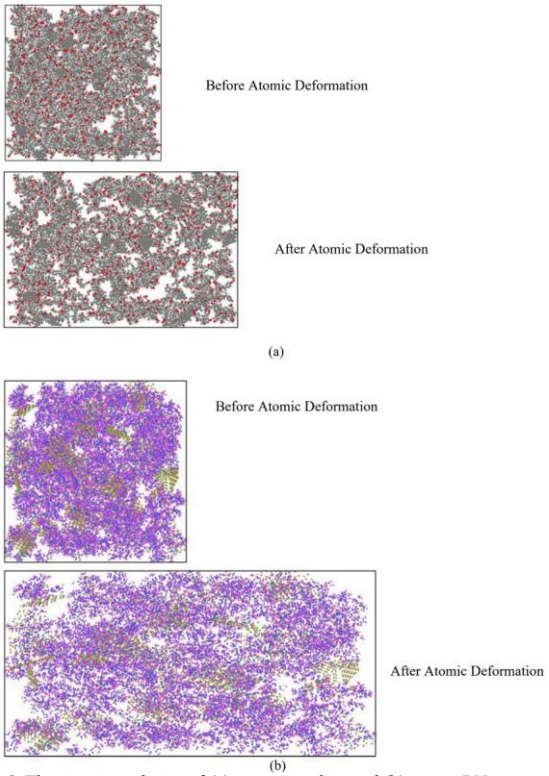

Fig. 6. The atomic evolution of (a) epoxy-graphite and (b) epoxy-BN nanocomposites in presence of defined external force.

ite and epoxy-BN nanocomposites. After mechanical deformation occur, physical parameters such as interaction energy and gauge factor calculated.

3. MD Simulation Results and Discussion

3.1. Equilibrium Phase of Modeled Samples

As reported before, we describe the electromechanical properties of epoxy-graphite and epoxy-BN nanocomposites after external force implementing to defined matrixes via MD approach. Initial temperature of modeled samples set to 300 K in this computational step. Before description of the electromechanical performance of modeled compounds, the equilibrium phase should be detected inside MD box. Figs. 2 and 3 show the temperature and energy variation of various systems as a function of MD time. As shown in Fig. 3, 10 ns is sufficient time to thermodynamic stability detected in epoxy-graphite and epoxy-BN nanocomposites. Structurally, this stability arises from convergence of atomic fluctuations amplitude by MD time passing. This evolution prevents the structural divergence of designed nanocomposites. Numerically, the potential energy value in defined structures converged to -7206.08 eV and -7563.85 eV for epoxy-graphite and epoxy-BN nanocomposites, respectively. The negative value of potential energy predicted the mean attraction force between particles in various regions of samples. After, equilibrium phase detection, we calculated the Radial Distribution Function (RDF) of total system to describe atomic arrangements of them [43]. Computationally, the RDF is a mathematical function used to describe the distribution of particles in an atomic structure. It quantifies the probability of finding a particle at a certain distance from a reference particle. The RDF results of equilibrated nanocomposites depicted in Fig. 4. These estimated results consistent with previous researches for solid structures and predicted computational settings validity in current research [43].

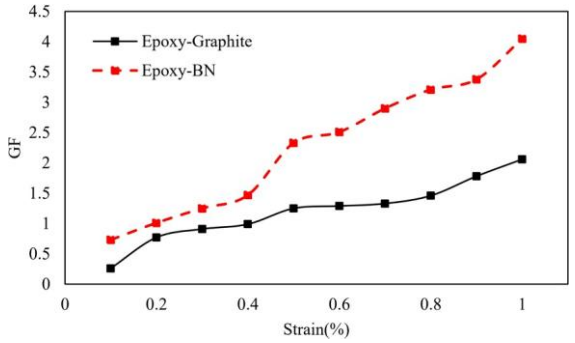

Fig. 7. The gauge factor variation of epoxy-graphite and epoxy-BN nanocomposites in presence of 1% graphite and BN nanoparticles.

3.2. Electromechanical Properties of Simulated Nanocomposites

Next, external force implemented to equilibrated epoxy-graphite and epoxy-BN nanocomposites to electromechanical study of them. After the equilibration state occur, the density value changes as a function simulation time at T_0=300 K calculated. MD outputs indicated the density of atomic nanocomposites converged to 1117 kg/m^3 and 1120 kg/m^3 for structures in presence of graphite and BN nanoparticles, as depicted in Fig. 5. From the density value converging process, it is concluded that the computational time is long enough to the nanocomposite sample reach to equilibrium condition. Furthermore, the density convergence in modeled sample predicted the consistency between modeled atomic structure and implemented force-fields to them. Subsequent to this computational step, the external force inserted to nanocomposites as depicted in Fig. 6. Theoretically, the gauge factor of defined structures can be described the electromechanical behavior of them (in presence of external force). From acquired computational results, the maximum ratio of this parameter reach to 2.06 and 4.05 for epoxy-graphite and epoxy-BN nanocomposites (respectively) in presence of 1% nanoparticle inside pristine matrix (see Fig. 7). Our calculated results in this section indicated graphite and BN nanoparticles appropriate behavior for electromechanical purposes. In comparison, the BN nanoparticles show more effective performance rather to graphite. This performance arises from polymeric chain evolution intensifies in presence of BN structure. So, polymeric chain displacements inside computational box occur effectively and gauge factor converged to larger value in epoxy-BN nanocomposite.

From previous reports, we conclude by nanoparticles atomic ratio changes, the atomic evolution and physical behavior of various nanocomposites can be optimized [44]. These optimum performances occur by appropriate nanoparticles distribution inside designed samples. In this step of our work, graphite and BN nanoparticles inserted to epoxy matrix with various ratio to improve pristine matrixes electromechanical properties. For described structures, nanoparticles atomic ratio set to 1%, 2%, 3%, 4.6% and 5%. After equilibration state detected, the atomic systems were deformed to introduce the electromechanical behavior of them. The gauge factor of various reinforced nanocomposites in the X direction is depicted in Fig. 8. Numerically, the maximum gauge factor in epoxy-graphite nanocomposite changes from 2.06 to 3.19 value as a function of nanoparticles ratio. Furthermore, this physical parameter reached to 6.54 by inserting 4.6% BN nanostructure to pristine matrix in epoxy-BN sample. Physically, by using optimum ratio of nanoparticles inside pristine epoxy matrix, the mean attraction force in various regions of samples maximized and structural changes of nanocomposite against external force converged to optimum state.

Finally, the interaction energy between nanoparticles and pristine epoxy matrix reported to more physical analysis of designed MD simulations. It is a measure of the attractive or repulsive forces between the

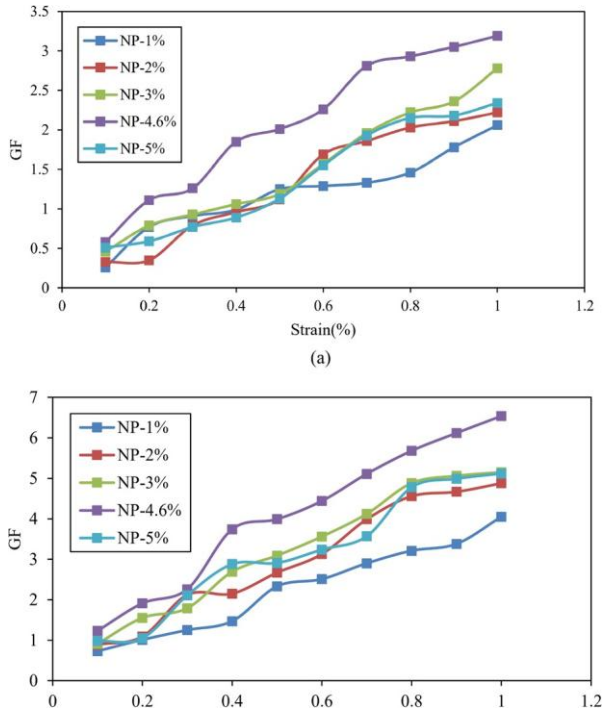

Fig. 8. The gauge factor changes of (a) epoxy-graphite and (b) epoxy-BN nanocomposites as a function of graphite and BN nanoparticles ratio inside pristine matrix.

particles and plays a crucial role in determining the overall stability and behavior of the system. This physical parameter show attraction forces between various parts of modeled samples. So, the structural unity occurs inside nanocomposites which caused mechanical strength detected in modeled nanocomposites against implemented external force. We listed the total component of this energy in Tables 2 and 3. MD results indicated by nanostructures ratio increasing to 4.6%, the interaction energy between nanostructure and matrix converged to -383.31 and -419.86 eV in presence of graphite and BN nanostructures, respectively (see Fig. 9). These numeric results indicated BN nanoparticles attracted intensely with polymeric matrix. Physically, more attraction force inside sample arises from more atomic consistent between pristine matrix and inserted nanoparticles. Finally, this behavior predicted more stability of epoxy-BN nanocomposite rather to epoxy-graphite matrix. So, we can say epoxy-BN nanocomposite is promising material for electromechanical applications.

4. Conclusions

In this computational work, we described the electromechanical behavior of epoxy-graphite and epoxy-BN nanocomposites at 300 K (initial condition). Current research done by using molecular dynamics (MD)

Table 3.
The gauge factor and interaction energy changes of reinforced epoxy-BN nanocomposite as a function of nanoparticles ratio.

Nanocomposite Atomic Ratio (%)	Gauge Factor	Interaction Energy (eV)
1	4.05	-392.00
2	4.88	-399.24
3	5.15	-405.19
4.6	6.54	-419.86
5	5.12	-402.06

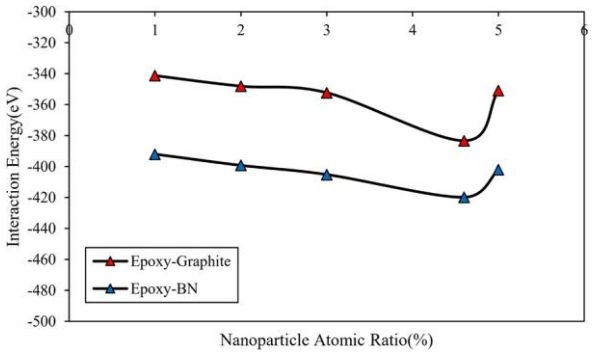

Fig. 9. The interaction energy variation of epoxy-graphite and epoxy-BN samples as a function of nanoparticles ratio.

method and LAMMPS package. Technically, the UFF, and TERSOFF force-fields has been implemented to MD simulation of epoxy-graphite and epoxy-BN nanocomposites. Simulation outputs indicated the atomic stability of defined structures by calculating temperature and potential energy parameters. Also, electromechanical behavior of epoxy-graphite and epoxy-BN nanocomposites reported by interaction energy and gauge factors calculations. Generally, MD simulation outputs in modeled nanocomposites can be listed as below,

1. The UFF and TERSOFF force-fields are appropriate performance to description of time evolution of epoxy-graphite and epoxy-BN nanocomposites.
2. The energy (potential) of defined compounds reached to -7206.08 and -7563.85 eV for epoxy-graphite and epoxy-BN nanocomposites after 10 ns. These convergences predicted the structural unity in designed nanocomposites.
3. By implementing external force to epoxy-graphite and epoxy-BN nanocomposites, these atomic systems expanded longitudinally.
4. The gauge factor of modeled epoxy-graphite and epoxy-BN nanocomposites converged to 2.06 and 4.05 values, respectively.
5. The gauge factor of modeled structures can be manipulated by nanoparticles atomic ratio changes. By using 4.5% graphite and BN inside MD box, the gauge factor of them converged to 3.19 and 6.54, respectively.
6. The interaction energy between nanoparticles and epoxy matrix varied from -383.31 eV to -419.86 eV by nanoparticles type and their atomic ratio changes.

Finally, we expected material designers improved the electromechanical efficiency of epoxy-based nanocomposites by using MD simulations outputs in actual applications.

Conflict of interest

The authors declare that they have no conflicts of interest

Acknowledgments

The authors acknowledge financial support from Babol Noshirvani University of Technology grant BNUT/370119/1402.

Authors' contributions

Peyman Torkian: Designed the analysis, Performed the analysis; Wrote the paper. **Hamid Baseri:** Designed the analysis, proof reading.

REFERENCES

[1] T.G. Beckwith, N.L. Buck, R. angoni, Mechanical measurements, Addison-Wesley New York1982.
[2] J. Bryzek, S. Roundy, B. Bircumshaw, C. Chung, K. Castellino, J.R. Stetter, M. Vestel, Marvelous MEMS, IEEE Circuits and Devices Magazine 22(2) (2006) 8-28.
[3] W.J. Westerveld, S.M. Leinders, P.M. Muilwijk, J. Pozo, T.C.v.d. Dool, M.D. Verweij, M. Yousefi, H.P. Urbach, Characterization of Integrated Optical Strain Sensors Based on Silicon Waveguides, IEEE Journal of Selected Topics in Quantum Electronics 20(4) (2014) 101-110.
[4] J. Carr, J. Baqersad, C. Niezrecki, P. Avitabile, M. Slattery, Dynamic Stress–Strain on Turbine Blades Using Digital Image Correlation Techniques Part 2: Dynamic Measurements, in: R. Mayes, D. Rixen, D.T. Griffith, D. De Klerk, S. Chauhan, S.N. Voormeeren, M.S. Allen (Eds.) Topics in Experimental Dynamics Substructuring and Wind Turbine Dynamics, Volume 2, Springer New York, New York, NY, 2012, pp. 221-226.
[5] J. Carr, J. Baqersad, C. Niezrecki, P. Avitabile, M. Slattery, Dynamic Stress–Strain on Turbine Blade Using Digital Image Correlation Techniques Part 1: Static Load and Calibration, in: R. Mayes, D. Rixen, D.T. Griffith, D. De Klerk, S. Chauhan, S.N. Voormeeren, M.S. Allen (Eds.) Topics in Experimental Dynamics Substructuring and Wind Turbine Dynamics, Volume 2, Springer New York, New York, NY, 2012, pp. 215-220.
[6] J.D. Littell, Large Field Photogrammetry Techniques in Aircraft and Spacecraft Impact Testing, in: T. Proulx (Ed.) Dynamic Behavior of Materials, Volume 1, Springer New York, New York, NY, 2011, pp. 55-67.
[7] M.C. Eble, F.I. Gonzalez, Deep-Ocean Bottom Pressure Measurements in the Northeast Pacific, Journal of Atmospheric and Oceanic Technology 8(2) (1991) 221-233.
[8] B.K.G. Theng, Formation and Properties of Clay-polymer Complexes, Elsevier Scientific Publishing Company 1979.
[9] Y. Lvov, B. Guo, R.F. Fakhrullin, Functional polymer composites with nanoclays, Royal Society of Chemistry 2016.
[10] A. Asgharinezhad, E. Niknam, A. Larimi, Simple synthesis of Fe_3O_4@Fe_3S_4 Nanocomposites coated with polyindole-polythiophene for high-performance supercapacitor, Journal of Composites and Compounds 5(14) (2023) 20-24.
[11] S. Mirzazadeh Khomambazari, P. Lokhande, S. Padervand, N.D. Zaulkiflee, M. Irandoost, S. Dubal, H. Sharifan, A review of recent progresses on nickel oxide/carbonous material composites as supercapacitor electrodes, Journal of Composites and Compounds 4(13) (2022) 195-208.
[12] H. Meskher, F. Achi, H. Belkhalfa, Synthesis and Characterization of CuO@PANI composite: A new prospective material for electrochemical sensing, Journal of Composites and Compounds 4(13) (2022) 178-181.
[13] S. Askari, Z.A. Bozcheloei, Piezoelectric composites in neural tissue engineering: material and fabrication techniques, Journal of Composites and Compounds 4(10) (2022) 37-46.
[14] P.M. Ajayan, L.S. Schadler, P.V. Braun, Nanocomposite Science and Technology, Wiley 2003.
[15] Z. Tian, H. Hu, Y. Sun, A molecular dynamics study of effective thermal conductivity in nanocomposites, International Journal of Heat and Mass Transfer 61 (2013) 577-582.
[16] M. Birkholz, U. Albers, T. Jung, Nanocomposite layers of ceramic oxides and metals prepared by reactive gas-flow sputtering, Surface and Coatings Technology 179(2) (2004) 279-285.
[17] D. Janas, B. Liszka, Copper matrix nanocomposites based on carbon nanotubes or graphene, Materials Chemistry Frontiers 2(1) (2018) 22-35.
[18] J.R. Garcia, D. O'Suilleabhain, H. Kaur, J.N. Coleman, A Simple Model Relating Gauge Factor to Filler Loading in Nanocomposite Strain Sensors, ACS Applied Nano Materials 4(3) (2021) 2876-2886.
[19] X. Ren, A.K. Chaurasia, A.I. Oliva-Avilés, J.J. Ku-Herrera, G.D. Seidel, F. Avilés, Modeling of mesoscale dispersion effect on the piezoresistivity of carbon nanotube-polymer nanocomposites via 3D computational multiscale micromechanics methods, Smart Materials and Structures 24(6) (2015) 065031.
[20] D. An, J. Nourry, S. Gharavian, V.K. Thakur, I. Aria, I. Durazo-Cardenas, T. Khaleque, H. Yazdani Nezhad, Strain self-sensing tailoring in functionalised carbon nanotubes/epoxy nanocomposites in response to electrical resistance change measurement, (2020).
[21] B.J. Alder, T.E. Wainwright, Studies in Molecular Dynamics. I. General Method, The Journal of Chemical Physics 31(2) (2004) 459-466.
[22] J.B. Gibson, A.N. Goland, M. Milgram, G.H. Vineyard, Dynamics of Radiation Damage, Physical Review 120(4) (1960) 1229-1253.
[23] A. Rahman, Correlations in the Motion of Atoms in Liquid Argon, Physical Review 136(2A) (1964) A405-A411.
[24] W.M. Brown, P. Wang, S.J. Plimpton, A.N. Tharrington, Implementing molecular dynamics on hybrid high performance computers – short range forces, Computer Physics Communications 182(4) (2011) 898-911.
[25] W.M. Brown, A. Kohlmeyer, S.J. Plimpton, A.N. Tharrington, Implementing molecular dynamics on hybrid high performance computers – Particle–particle particle-mesh, Computer Physics Communications 183(3) (2012) 449-459.
[26] S. Plimpton, Fast Parallel Algorithms for Short-Range Molecular Dynamics, Journal of Computational Physics 117(1) (1995) 1-19.
[27] L. Martínez, R. Andrade, E.G. Birgin, J.M. Martínez, PACKMOL: A package for building initial configurations for molecular dynamics simulations, Journal of Computational Chemistry 30(13) (2009) 2157-2164.
[28] M.D. Hanwell, D.E. Curtis, D.C. Lonie, T. Vandermeersch, E. Zurek, G.R. Hutchison, Avogadro: an advanced semantic chemical editor, visualization, and analysis platform, Journal of Cheminformatics 4(1) (2012) 17.
[29] A.R. Leach, Molecular modelling: principles and applications, Pearson education 2001.
[30] A.K. Rappe, C.J. Casewit, K.S. Colwell, W.A. Goddard, III, W.M. Skiff, UFF, a full periodic table force field for molecular mechanics and molecular dynamics simulations, Journal of the American Chemical Society 114(25) (1992) 10024-10035.
[31] J. Tersoff, New empirical approach for the structure and energy of covalent systems, Physical Review B 37(12) (1988) 6991-7000.
[32] D.W. Brenner, Relationship between the embedded-atom method and Tersoff potentials, Physical Review Letters 63(9) (1989) 1022-1022.
[33] J.E. Lennard-Jones, Cohesion, Proceedings of the Physical Society 43(5) (1931) 461.
[34] R.A. Serway, J.W. Jewett, Physics for Scientists and Engineers (with PhysicsNOW and InfoTrac), Brooks Cole Monterey, CA, 2003.
[35] P.A. Tipler, G. Mosca, Physics for scientists and engineers, Macmillan2007.
[36] D.C. Rapaport, R.L. Blumberg, S.R. McKay, W. Christian, The Art of Molecular Dynamics Simulation, Computer in Physics 10(5) (1996) 456-456.
[37] S. Nosé, A unified formulation of the constant temperature molecular dynamics methods, The Journal of Chemical Physics 81(1) (1984) 511-519.
[38] W.G. Hoover, Canonical dynamics: Equilibrium phase-space distributions, Physical Review A 31(3) (1985) 1695-1697.
[39] L. Verlet, Computer "Experiments" on Classical Fluids. I. Thermodynamical Properties of Lennard-Jones Molecules, Physical Review 159(1) (1967) 98-103.
[40] W. Press, S. Teukolsky, W. Vetterling, B. Flannery, Section 17.4. Second-order conservative equations, Numerical recipes: The art of scientific computing, 3rd ed., Cambridge University Press, New York (2007).
[41] E. Hairer, C. Lubich, G. Wanner, Geometric numerical integration illustrated by the Störmer–Verlet method, Acta Numerica 12 (2003) 399-450.
[42] W. Mai, P. Li, H. Bao, X. Li, L. Jiang, J. Hu, D.H. Werner, Prism-Based DGTD With a Simplified Periodic Boundary Condition to Analyze FSS With D2n Symmetry in a Rectangular Array Under Normal Incidence, IEEE Antennas and Wireless Propagation Letters 18(4) (2019) 771-775.
[43] R.E. Dinnebier, S.J. Billinge, Powder diffraction: theory and practice, Royal society of chemistry 2008.
[44] L. Zhao, M.K.M. Nasution, M. Hekmatifar, R. Sabetvand, P. Kamenskov, D. Toghraie, A.a. Alizadeh, T.G. Iran, The improvement of mechanical properties of conventional concretes using carbon nanoparticles using molecular dynamics simulation, Scientific Reports 11(1) (2021) 20265.